A&A 414, 335–350 (2004)
DOI: 10.1051/0004-6361:20031605

Astronomy & Astrophysics

Dust in brown dwarfs

III. Formation and structure of quasi-static cloud layers

P. Woitke[1] and Ch. Helling[1,2]

[1] Zentrum für Astronomie und Astrophysik, Technische Universität Berlin, Hardenbergstraße 36, 10623 Berlin, Germany
[2] Konrad-Zuse-Zenrum für Informationstechnik Berlin, Takustraße 7, 14195 Berlin, Germany

Received 26 March 2003 / Accepted 13 October 2003

Abstract. In this paper, first solutions of the dust moment equations developed in (Woitke & Helling 2003) for the description of dust formation and precipitation in brown dwarf and giant gas planet atmospheres are presented. We consider the special case of a static brown dwarf atmosphere, where dust particles continuously nucleate from the gas phase, grow by the accretion of molecules, settle gravitationally and re-evaporate thermally. Mixing by convective overshoot is assumed to replenish the atmosphere with condensable elements, which is necessary to counterbalance the loss of condensable elements by dust formation and gravitational settling (no dust without mixing). Applying a kinetic description of the relevant microphysical and chemical processes for TiO_2-grains, the model makes predictions about the large-scale stratification of dust in the atmosphere, the depletion of molecules from the gas phase, the supersaturation of the gas in the atmosphere as well as the mean size and the mass fraction of dust grains as function of depth. Our results suggest that the presence of relevant amounts of dust is restricted to a layer, where the upper boundary (cloud deck) is related to the requirement of a minimum mixing activity (mixing time-scale $\tau_{\rm mix} \approx 10^6$ s) and the lower boundary (cloud base) is determined by the thermodynamical stability of the grains. The nucleation occurs around the cloud deck where the gas is cool, strongly depleted, but nevertheless highly supersaturated ($S \gg 1$). These particles settle gravitationally and populate the warmer layers below, where the in situ formation (nucleation) is ineffective or even not possible. During their descent, the particles grow and reach mean radii of $\approx 30\,\mu$m ... $400\,\mu$m at the cloud base, but the majority of the particles in the cloud layer remains much smaller. Finally, the dust grains sink into layers which are sufficiently hot to cause their thermal evaporation. Hence, an effective transport mechanism for condensable elements exists in brown dwarfs, which depletes the gas above and enriches the gas below the cloud base of a considered solid/liquid material. The dust-to-gas mass fraction in the cloud layer results to be approximately given by the mass fraction of condensable elements in the gas being mixed up. Only for artificially reduced mixing we find a self-regulation mechanism that approximately installs phase equilibrium ($S \approx 1$) in a limited region around the cloud base.

Key words. stars: atmospheres – stars: low-mass, brown dwarfs – dust, extinction – molecular processes – methods: numerical

1. Introduction

For ultra-cool stars and giant gas planets, the classical theory of stellar atmospheres suffers from the lack of a reliable theory for the formation of solid particles and fluid droplets (henceforth called *dust*) in the atmosphere with are important opacity carriers. A standard method to predict the amount and the size distribution of dust particles of different kinds as function of depth, and their influence on the abundances in the atmosphere is not yet at hand.

Static model atmosphere calculations for brown dwarfs with frequency-dependent radiative transfer and mixing-length theory (e.g. Allard et al. 2001; Burrows et al. 2002; Marley et al. 2002; Tsuji 2002) have, therefore, mainly used ad hoc *assumptions* for the treatment of the dust component so far. Depending on the purpose of the model, the dust is simply disregarded, the dust is assumed to be fully condensed and present or to have rained out, leaving behind a saturated, i.e. strongly metal-deficient atmosphere. In each case, the spectral appearance of molecular bands in the calculated spectra and the structure of the atmosphere results to be quite different, which underlines the necessity of a consistent modelling of the dust component in brown dwarf atmospheres.

The formation and precipitation of dust particles has furthermore been suggested to cause the observed evolutionary sequence from L to T dwarfs, which change their $J-K$ colour from red to blue with increasing age (Kirkpatick et al. 1999; Marley et al. 2002; Burgasser et al. 2002). As the brown dwarfs evolve along their cooling trajectory, the active dust forming regions are suggested to sink below the photospheric level due to temperature constraints, which causes the star to emit bluer than at earlier ages, when the effective temperature was higher.

Send offprint requests to: P. Woitke,
e-mail: woitke@astro.physik.tu-berlin.de

Thus, a strong need exists for a more profound modelling of the dust component in ultra-cool stellar atmospheres. In particular, the dust size distribution has often been treated inattentively in the models so far, e.g. using the distribution function of the interstellar medium (e.g. Allard et al. 2001). Several works have addressed this problem (e.g. Lunine et al. 1989; Ackermann & Marley 2001; Cooper et al. 2003) and have arrived at some first-order solutions. These works are guided by stability considerations and follow a decision tree based on the local time-scale arguments of Rossow (1978), which are originally based on the experience with the earth's atmosphere. However, these works do not aim at a kinetic description of the underlying microphysical and chemical processes.

In Woitke & Helling (2003, hereafter Paper II), a time-dependent physical description of the dust component in brown dwarf atmospheres has been developed by extending the classical dust moment method developed by Gail & Sedlmayr (1988), Gauger et al. (1990) and Dominik et al. (1993) to include size-dependent particle drift. Two different systems of partial differential equations in conservation form have been derived for the two relevant limiting cases of small Knudsen numbers (subsonic free molecular flow) and large Knudsen numbers (laminar flow). These equations offer a unique method to simultaneously model nucleation, growth, evaporation, element consumption and gravitational settling of heterogeneous grains.

In this paper, we aim at a first application of this method in the frame of a static atmosphere. We are mainly interested in the physical control mechanisms that are responsible for the formation and the structure of a quasi-static cloud layer. As example for refractory grains, we solve the dust moment equations for TiO_2-grains for the special case of a prescribed plane-parallel atmospheric gas stratification, where dust particles continuously form, settle gravitationally and evaporate, i.e. we assume that the dust component is stationary. In this stationary case, the downward directed element transfer via precipitating dust grains is balanced by an upward directed flux of condensable elements from the deep interior of the star via mixing by convective overshoot. This basic scenario has already been proposed by Helling et al. (2001b) and Ackerman & Marley (2001). We summarise the extended dust moment equations and derive their special form for the plane-parallel, static, stationary case in Sect. 2, along with a short description of the applied boundary and closure conditions, and our numerical method to solve the resulting system of ordinary differential equations. In Sect. 3, the calculated vertical structures of quasi-static cloud layers in brown dwarf atmospheres are presented. We discuss these results with respect to previous works in Sect. 4. Our conclusions are outlined in Sect. 5.

2. The model of a quasi-static cloud layer

In the following, we apply the kinetic description for nucleation, growth, evaporation, and gravitational settling of dust grains as developed in Paper II to a quasi-static brown dwarf atmosphere. We consider the subsonic, large Knudsen number case (lKn = {Kn $\gg$ 1 and $|\boldsymbol{v}_{\rm dr}| \ll c_{\rm T}$}, compare Paper II), because – as the results will show – the majority of dust grains building up the cloud layer fall into this regime[1]. For this special case, the following system of dust moment equations has been derived in Paper II:

$$\frac{\partial}{\partial t}\Big(\rho L_j\Big) + \nabla\cdot(\boldsymbol{v}_{\rm gas}\,\rho L_j) = V_\ell{}^{j/3} J(V_\ell) + \frac{j}{3}\chi^{\rm net}_{\rm lKn}\,\rho L_{\rm j-1} + \xi_{\rm lKn}\nabla\left(\frac{L_{j+1}}{c_{\rm T}}\,\boldsymbol{e}_r\right) \quad (1)$$

$$\text{with}\quad \chi^{\rm net}_{\rm lKn} = \sqrt[3]{36\pi}\sum_{r=1}^{R}\Delta V_r\, n_r v_r^{\rm rel}\alpha_r\left(1-\frac{1}{S_r}\right) \quad (2)$$

$$\xi_{\rm lKn} = \frac{\sqrt{\pi}}{2}\left(\frac{3}{4\pi}\right)^{1/3} g\rho_{\rm d}. \quad (3)$$

$\rho L_j = \int_{V_\ell}^{\infty} f(V) V^{j/3}\,{\rm d}V$ [cm^{j-3}] ($j = 0, 1, 2, ...$) is the jth moment of the grain size distribution function in volume space $f(V)$ [cm^{-6}], $\chi^{\rm net}_{\rm lKn}$ [cm/s] is the net growth speed, $\xi_{\rm lKn}$ [dyn cm^{-3}] the drag force density, n_r [cm^{-3}] the particle density of the key species of surface reaction r in the gas phase and S_r its generalised supersaturation ratio. For more details about Eqs. (1)–(3) please consult Paper II.

The element depletion is taken into account by evaluating the consumption of each involved element i with relative abundance to hydrogen ϵ_i by nucleation and growth

$$\frac{\partial}{\partial t}\Big(n_{\langle\rm H\rangle}\epsilon_i\Big) + \nabla\cdot\Big(\boldsymbol{v}_{\rm gas}\, n_{\langle\rm H\rangle}\epsilon_i\Big) = -\nu_{i,0}\, N_\ell\, J(V_\ell) - \sqrt[3]{36\pi}\rho L_2\sum_{r=1}^{R}\nu_{i,r}\, n_r v_r^{\rm rel}\alpha_r\left(1-\frac{1}{S_r}\right) \quad (4)$$

with stoichiometric ratios of homogeneous nucleation $\nu_{i,0}$ and surface reactions $\nu_{i,r}$. $n_{\langle\rm H\rangle}$ is the total hydrogen nuclei density ($\rho = 1.427$ amu $n_{\langle\rm H\rangle}$ for solar abundances).

In the following, we assume a quasi-static atmosphere ($\boldsymbol{v}_{\rm gas} = 0$), plane-parallel geometry ($\boldsymbol{e}_r = \boldsymbol{e}_z$), constant gravity ($g = $ const) and a stationary dust component ($\frac{\partial L_j}{\partial t} = 0$). In this special case, the system of moment Eq. (1) degenerates into a system of ordinary differential equations ($j = 0, 1, 2, ...$)

$$V_\ell{}^{j/3} J(V_\ell) + \frac{j}{3}\chi^{\rm net}_{\rm lKn}\,\rho L_{j-1} + \xi_{\rm lKn}\frac{\rm d}{{\rm d}z}\left(\frac{L_{j+1}}{c_{\rm T}}\right) = 0. \quad (5)$$

In the static stationary case, the element consumption equations turn into algebraic equations for each element i

$$\nu_{i,0}\, N_\ell\, J(V_\ell) + \sqrt[3]{36\pi}\rho L_2\sum_{r=1}^{R}\nu_{i,r} n_r v_r^{\rm rel}\alpha_r\left(1-\frac{1}{S_r}\right) = 0. \quad (6)$$

2.1. Treatment of convective mixing

As shown in Appendix A, the coupled system of dust moment and element consumption equations in the static stationary case

[1] Small Knudsen numbers may in fact occur in the innermost layers around the cloud base, where the gas densities are highest and the dust grains are largest (see Sect. 4.1). According to the purpose of this paper, we will nevertheless avoid at first the troublesome Knudsen number fall differentiation as proposed in Paper II.

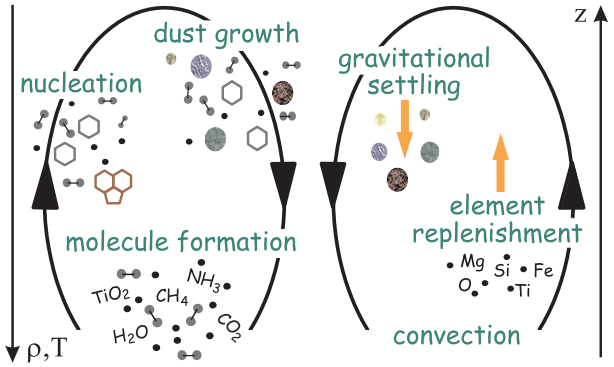

Fig. 1. Sketch of the convective dust formation: Life cycle of dust grains in sub-stellar atmospheres.

(Eqs. (5) and (6)) has only a trivial solution. According to this solution, a truly static atmosphere must be completely dust-free $L_j = 0$ and cannot be supersaturated anywhere $S_r \leq 1$. The physical interpretation of this trivial solution is that dust grains, which have once formed in the sufficiently cool layers, have consumed all available condensable elements up to the saturation level, and have finally left the model volume by gravitational settling.

This picture changes, however, if we take into account a mixing of the atmosphere caused by the convection. This mixing leads to an ongoing replenishment of the gas with fresh, uncondensed matter from the deep interior of the brown dwarf, which can counterbalance the loss of condensable elements via the formation and gravitational settling of dust grains. Thus, a convective mixing can maintain the stationary situation sketched in Fig. 1: Seed particles nucleate in metal-rich, i.e. supersaturated upwinds. Dust particles grow on top of these nuclei by the accretion of molecules and rain out as soon as they have reached a certain size. The sinking grains will finally reach deeper atmospheric layers which are hot enough to cause their thermal evaporation, which completes the life cycle of a dust grain in a brown dwarf atmosphere.

We therefore enlarge our model by a simple description of the convective mixing

$$-\frac{\mathrm{d}}{\mathrm{d}z}\left(\frac{L_{j+1}}{c_T}\right) = \frac{1}{\xi_{\mathrm{lKn}}}\left(-\frac{\rho L_j}{\tau_{\mathrm{mix}}} + V_\ell{}^{j/3} J_\star + \frac{j}{3}\chi^{\mathrm{net}}_{\mathrm{lKn}}\rho L_{j-1}\right) \qquad (7)$$

with algebraic auxiliary conditions

$$\frac{n_{\langle\mathrm{H}\rangle}(\epsilon_i^0 - \epsilon_i)}{\tau_{\mathrm{mix}}} = \nu_{i,0}\, N_\ell\, J_\star + \sqrt[3]{36\pi}\,\rho L_2 \sum_{r=1}^{R} \nu_{i,r} n_r v_r^{\mathrm{rel}} \alpha_r \left(1 - \frac{1}{S_r}\right). \qquad (8)$$

According to this approach, the gas/dust mixture in the atmosphere is continuously replaced by dust-free gas of solar abundances on a depth-dependent mixing time-scale $\tau_{\mathrm{mix}}(z)$, which can be adapted to a convection model. ϵ_i is the actual abundance of element i in the gas phase and ϵ_i^0 its solar value (Anders & Grevesse 1989). We have chosen this simple description of the mixing in accordance with the purpose of this paper to concentrate on the dust processes responsible for the formation and structure of quasi-static cloud layers. A more sophisticated description for the mixing, assuming a quasi-diffusive character, is discussed in Sect. 4.2.

Brown dwarfs are known to be almost fully convective (Chabrier & Baraffe 1997), but the outermost layers of the atmosphere with $T \lesssim 2000\,\mathrm{K}$ are radiative (e.g. Tsuji 2002). Therefore, at a first glance, the existence of dust seems impossible in brown dwarf atmospheres, since the convectively unstable regions are too hot and the cooler regions above are not mixed. However, the hydrodynamic motions excited in the convectively unstable zone do not stop abruptly at its outer boundary. Driven by their inertia, ascending bubbles penetrate much higher into the radiative layers, a phenomenon commonly denoted as *overshooting*. This overshooting leads to a strongly reduced but non-vanishing mixing even a few scale heights above the convection zone (e.g. Freytag et al. 1996).

In order to determine $\tau_{\mathrm{mix}}(z)$ we adopt the horizontally and time-averaged results of 3D dynamical simulations of the surface convection by Ludwig et al. (2002). These models show that, generally speaking, the convectively excited hydrodynamical motions – and thereby the mixing – decay only moderately with increasing height above the convectively unstable zone. In consideration of M-dwarfs, Ludwig et al. (2002) have proposed to fit this behaviour by an exponential decrease of the mass exchange frequency f_{exchange} in the radiative zone. We follow their approach and use the following rough description of the mixing

$$\log\tau_{\mathrm{mix}}(z) = \log\tau^{\mathrm{min}}_{\mathrm{mix}} + \beta\cdot\max\Big\{0\,,\ \log p_0 - \log p(z)\Big\}. \qquad (9)$$

p_0 is the pressure at the upper edge of the convectively unstable zone (defined by the Schwarzschild criterion), $\tau^{\mathrm{min}}_{\mathrm{mix}}$ the minimum value of the mixing time-scale occurring in the convectively unstable region and $\beta = \Delta\log f_{\mathrm{exchange}}/\Delta\log p \approx 2.2$ the logarithmic slope as measured from Fig. 16 of Ludwig et al. (2002), which roughly scales as $\beta \propto g^{1/2}$ for M-type atmospheres (Ludwig 2003). Preliminary results from hydrodynamical models of lower effective temperatures show a comparable degree of overshoot (Ludwig 2003, priv. comm.). In order to determine the minimum mixing time-scale, we assume $\tau^{\mathrm{min}}_{\mathrm{mix}} = \mathrm{const.}\, H_{\mathrm{p}}/v^{\mathrm{max}}_{\mathrm{cnv}}$ and adopt the maximum convective velocities derived from mixing length theory by Tsuji (2002): $v^{\mathrm{max}}_{\mathrm{cnv}} \approx 40\,\mathrm{m\,s^{-1}}$, $30\,\mathrm{m\,s^{-1}}$, $20\,\mathrm{m\,s^{-1}}$ for $\log g = 5$ and $T_{\mathrm{eff}} = 1800\,\mathrm{K}$, $1400\,\mathrm{K}$, $1000\,\mathrm{K}$, respectively[2]. The proportionality constant const is calculated from the results of Ludwig et al. (2002): $\tau^{\mathrm{min}}_{\mathrm{mix}} \approx 100\,\mathrm{s}$ for $v^{\mathrm{max}}_{\mathrm{cnv}} \approx 200\,\mathrm{m\,s^{-1}}$, $\log g = 5$ and $T_{\mathrm{eff}} = 2790\,\mathrm{K}$. This procedure leads to values $\tau^{\mathrm{min}}_{\mathrm{mix}} = 320\,\mathrm{s}$, $330\,\mathrm{s}$, $360\,\mathrm{s}$ for $\log g = 5$ and $T_{\mathrm{eff}} = 1800\,\mathrm{K}$, $1400\,\mathrm{K}$, $1000\,\mathrm{K}$, respectively. In order to keep our models as simple and comparable as possible, we simply adopt a unique value here: $\tau^{\mathrm{min}}_{\mathrm{mix}} = 300\,\mathrm{s}$.

In Eqs. (7) and (8), we have furthermore replaced $J(V_\ell)$ by the nucleation rate $J_\star$. While both terms are in fact nearly equal in the supersaturated case $S > 1$ (Gail & Sedlmayr 1988), this is an approximation in the undersaturated case, where all

[2] In comparison to the Ludwig et al. models, these values are rather small. Ludwig et al. (2002) note that rather large values for the mixing length parameter α must be used to fit the convective velocities in their dynamical models.

particles evaporate. Here, $J(V_\ell) = f(V_\ell)\frac{\mathrm{d}V}{\mathrm{d}t}\big|_{V=V_\ell}$ should be calculated from the actual cluster size distribution function at the lower boundary $f(V_\ell)$ and its volume decrement $\frac{\mathrm{d}V}{\mathrm{d}t}\big|_{V=V_\ell} < 0$. Unfortunately, $f(V_\ell)$ is not known[3], so we use $J(V_\ell) = J_\star$ as a simplifying approximation which underestimates the influence of evaporation on the dust moments. However, as the results will show, the gravitationally settling dust grains evaporate very quickly, which affects only a thin layer below the cloud base.

2.2. Application to TiO_2

Only one example dust species will be considered in the following, i.e. we assume that the dust particles are composed of a unique material, again to keep the model as transparent as possible. The following complications would arise if different kinds of condensates were considered simultaneously: (i) Dust grains of different kinds may condensate independently, competing for the remaining condensable elements in the gas phase. (ii) One solid species may provide the seed particles for another solid species to condense at its surface *(core-mantle grains)*. (iii) Two or more solid species may condense simultaneously on the same surface to form *dirty grains*. These details, which would considerably complicate the understanding of the stationary behaviour of the dust component, are disregarded here, but will be addressed in a future paper[4].

As exemplary solid species, typical for refractory grains, we choose *rutile* TiO_2[s] because (i) it is among the thermodynamically most stable solid materials known and (ii) the monomer (the TiO_2 molecule) is abundant in the gas phase according to chemical equilibrium (e.g. Allard et al. 2001). Therefore, the formation of TiO_2 seed particles from the gas phase can be assumed to proceed via a stepwise addition of TiO_2 molecules to $(TiO_2)_N$ clusters (Jeong 2000), usually denominated as *homogeneous nucleation*. Therefore, classical nucleation theory can be applied to calculate the nucleation rate $J_\star$. In contrast, other high temperature condensates like corundum (Al_2O_3[s]) often have no stable monomer in the gas phase (Patzer et al. 1998) and the nucleation of such species seems questionable since three or more body collisions would be required to form small clusters of that kind in the gas phase. It seems more likely, that the condensation of materials like Al_2O_3 already requires the existence of some surface, e.g. the presence of seed particles provided by homogeneously nucleating species, as for example TiO_2.

For the growth and evaporation of macroscopic rutile dust particles, the following two chemical surface reactions are considered

$$\begin{aligned} \mathrm{TiO_2} + (\mathrm{TiO_2[s]})_N &\rightleftharpoons (\mathrm{TiO_2[s]})_{N+1} \qquad (r = 1) \\ \mathrm{TiO} + \mathrm{H_2O} + (\mathrm{TiO_2[s]})_N &\rightleftharpoons (\mathrm{TiO_2[s]})_{N+1} + \mathrm{H_2}\,(r = 2). \end{aligned} \tag{10}$$

The key species for reaction $r = 1$ is obviously $n_1 = n_{\mathrm{TiO_2}}$. Because of the small titanium abundance, the rate of reaction $r = 2$ is limited by the TiO number density in the gas phase and hence its key species is identified as $n_2 = n_{\mathrm{TiO}}$. Since both reactions transform one unit of the solid material, the volume increment is $\Delta V_1 = \Delta V_2 = \Delta V_{\mathrm{TiO_2}}$ and we assume $S_1 = S_2 = S_{\mathrm{TiO_2}}$ (see Paper II). Furthermore, we have $R = 2$, $i = 1$ for titanium and $i = 2$ for oxygen, $\nu_{1,0} = \nu_{1,1} = \nu_{1,2} = 1$ and $\nu_{2,0} = \nu_{2,1} = \nu_{2,2} = 2$.

The homogeneous nucleation rate $J_\star$ of $(TiO_2)_N$ clusters is calculated by applying modified classical nucleation theory according to the scheme of Gail et al. (1984) with parameters $\sigma^{\mathrm{TiO_2}} = 620\,\mathrm{erg/cm^2}$ and $N_f^{\mathrm{TiO_2}} = 0$ (Jeong 2000). These parameters, including the "surface tension" σ, result from a fit to quantum mechanical ab initio calculations (density functional theory) for *small* TiO_2 clusters (Jeong et al. 2000), which differ from the properties of the bulk phase.

The following data completes the problem. The monomer volume $\Delta V_{\mathrm{TiO_2}} = 3.135 \times 10^{-23}\,\mathrm{cm^{-3}}$ results from the rutile density $\rho_\mathrm{d} = 4.23\,\mathrm{g\,cm^{-3}}$ and its monomer weight $m_{\mathrm{TiO_2}} = 79.90$ amu. $\alpha_r = 1$ and $N_\ell = 1000$ are assumed. The saturation vapour pressure $p^{\mathrm{vap}}_{\mathrm{TiO_2}}(T)$ has been fitted to the JANAF-tables (1985, electronic version) such that the supersaturation ratio of rutile can be expressed by

$$S_{\mathrm{TiO_2}} = \frac{n_{\mathrm{TiO_2}} kT \ \left[\mathrm{dyn\,cm^{-2}}\right]}{\exp(35.8027 - 74734.7/T)}. \tag{11}$$

2.3. Prescribed atmospheric structure

As underlying atmospheric gas stratification, $T(p)$ and $\rho(p)$, we adopt three model structures for brown dwarf atmospheres for $\log g = 5$ and effective temperatures $T_\mathrm{eff} = 1000\,\mathrm{K}$, $1400\,\mathrm{K}$ and $1800\,\mathrm{K}$, kindly provided by *T*. Tsuji (2002). p is the thermal gas pressure. These reference models have been calculated by means of the standard assumptions of classical stellar atmospheres (planparallel geometry, hydrostatic equilibrium, frequency-dependent radiative transfer, mixing length theory, micro-turbulence broadening). We adopt his "case A"-models, where dust formation is ignored. Although obviously relevant, the properties of the calculated TiO_2 dust particles have, technically speaking, no influence on the adopted atmospheric structure in this paper. A consistent treatment of atmosphere and cloud structure would be advisable (certainly possible by simultaneously solving the equations for hydrostatic equilibrium, radiative transfer, convection and dust-chemistry), but is not carried out in this paper.

2.4. Numerical methods

2.4.1. Closure condition

The system of moment equations (Eq. (7)) is not closed, since L_0 appears on the r.h.s., whereas the equations are solved for L_{j+1} $(j = 0, 1, 2, ...)$ only. A solution of such an open moment system is only possible if a physically reasonable and numerically stable closure condition of the form $\mathcal{F}(L_0, L_1, L_2, L_3, ...) = 0$ can be provided. For numerical

[3] The numerical scheme proposed by Gauger et al. (1990) to reconstruct the size distribution function from the history of $J_\star$ and $\chi^{\mathrm{net}}_{\mathrm{1Kn}}$ in each gas element, cannot be applied here, since position coupling is not valid.

[4] Eqs. (1)–(3) are formulated for dirty grains, i.e. it is possible to discuss these questions by means of these equations.

reasons, this closure conditions should be fast, e.g. preferably analytical and invertible concerning L_0.

We have tested seven different approaches for this closure condition, including the scheme of (Deuflhard & Wulkow 1989; Wulkow 1992) in application to different weight functions $\Psi^\alpha(V)$ (see Paper II). In general, the solutions obtained with different approaches are very similar, but the convergence of the model may fail for certain choices of the closure condition, in particular regarding the undersaturated layers below the cloud base. In the following, we only describe a very simple but stable scheme, which is based on the experience that the dust moments can reasonably well be approximated by a power-law as function of the index j in most cases,

$$y(j) = A\, j^B \qquad \text{with} \qquad y(j) = \frac{L_j}{L_{j-1}}. \tag{12}$$

Given the moments L_j for $j \in \{1, 2, 3\}$, the coefficient A and the exponent B can be expressed by

$$A = \frac{L_2}{L_1\, 2^B} \qquad \text{and} \qquad B = \frac{\log\left(L_1 L_3 / L_2^2\right)}{\log(3/2)}, \tag{13}$$

and the desired equation for the 0th dust moment reads

$$L_0 = \frac{L_1}{A}. \tag{14}$$

This closure condition has proven to be most successful. Since L_0 is expressed in terms of L_1, L_2 and L_3 via Eqs. (13) and (14), the dust moment equations (Eq. (7)) only need to be solved for $j = 0, 1, 2$.

2.4.2. Boundary condition

The negative sign on the l.h.s. of Eq. (7) suggests an inward rather than an outward integration, naturally tracing the drift motion of the grains. We therefore integrate Eq. (7) *inward*, starting from an outer boundary $z_{\max}$, for which boundary conditions must be fixed. We assume that the atmosphere is dust-free at the outer boundary

$$L_j(z = z_{\max}) = 0, \tag{15}$$

which is true for vanishing mixing high above the convection zone (see Appendix A). The numerical solutions are found to be only marginally affected by the position of the outer boundary, as long as it is located well above (typically 10 scale heights above) the $P = 1$ bar level.

2.4.3. Algebraic equations and chemical equilibrium

The element consumption equations (Eq. (8)) are algebraic auxiliary conditions for each element i, which are coupled to the calculation of the molecular concentrations, the supersaturation ratio and the nucleation rate, and depend on the total surface area of the dust component ($\propto \rho L_2$). In our example, two equations have to be solved for $i = 1$ (titanium) and $i = 2$ (oxygen).

This system of non-linear algebraic equations is solved by iteration in each layer z prior to the evaluation of the r.h.s. terms of the differential equations (Eq. (7)). Given $n_{\langle \mathrm{H} \rangle}(z)$, $T(z)$, $\tau_{\mathrm{mix}}(z)$ and $L_2(z)$, the unknowns $\epsilon_i'(z)$ are estimated and all particle densities $n_k(z)$ (atoms, electrons, ions and molecules) are calculated in chemical equilibrium. Elements other than Ti and O are assumed to have solar abundances. We use 14 elements (H, He, C, N, O, Si, Mg, Al, Fe, S, Na, K, Ti, Ca) and 155 molecules in our chemical equilibrium code with equilibrium constants fitted to the thermodynamical molecular data from the electronic version of the JANAF tables (Chase et al. 1985). First ionisation states of all elements are sufficient to calculate reliable molecular concentrations also at higher temperatures (see discussion in Helling et al. 2000). From these particle densities, the supersaturation ratio $S_{\mathrm{TiO_2}}(z)$ and the nucleation rate $J_\star(z)$ are calculated, and the remaining errors in the auxiliary conditions (Eq. (8)) are quantified. A Newton-Raphson iteration is finally applied to find the root $\epsilon_i(z)$ of Eq. (8).

2.4.4. Numerical integration

The dust moment equations (Eq. (7)) for $j = 0, 1, 2$, completed by the equation of hydrostatic equilibrium $\mathrm{d}p/\mathrm{d}z = -\rho g$, form a system of four ordinary differential equations of first order which can be solved by standard numerical methods. The differential equations are integrated inward by means of the variable transformation $z' = z_{\max} - z$ using the RADAU 5 – solver for stiff ordinary differential equations (Hairer & Wanner 1991). The integration is stopped as soon as one of the dust moments becomes negative, indicating that the dust has completely evaporated.

3. Results

The calculated structures of the TiO_2 dust layer in brown dwarf atmospheres with $\log g = 5$ are depicted in Figs. 2 and 3, considering a sequence of models with increasing effective temperature $T_{\mathrm{eff}} = 1000\,\mathrm{K}$, 1400 K and 1800 K. In each case, the 1st panel shows the adopted static model structure (temperature and mixing time-scale) and panels 2–5 depict the calculated dust and gas properties which result from the consistent solution of the dust moment and element conservation equations.

Before we discuss these structures in detail, some general features of the models (see Table 1) shall be described first. The dust particles result to be present mainly in a restricted layer with smooth boundaries. Applying a 1σ-criterion for the degree of condensation,

$$\text{cloud layer} \quad \Longleftrightarrow \quad f_{\mathrm{cond}}^{\mathrm{Ti}} = \frac{\epsilon_{\mathrm{Ti}}^{\mathrm{dust}}}{\epsilon_{\mathrm{Ti}}^{0}} > \frac{1}{e}, \tag{16}$$

the layers have a geometrical thickness between $3\,H_{\mathrm{p}}$ and $4.5\,H_{\mathrm{p}}$. $\epsilon_{\mathrm{Ti}}^{\mathrm{dust}} = \rho L_3 / (n_{\langle \mathrm{H} \rangle} \Delta V_{\mathrm{TiO_2}})$ is the Ti abundance contained in the solid phase and $\epsilon_{\mathrm{Ti}}^{0}$ the Ti abundance in the gas being mixed up (solar value).

The upper boundary of the cloud layer, hereafter called *cloud deck*, is defined by the $f_{\mathrm{cond}}^{\mathrm{Ti}} = 1/e$ – criterion. It is found to be physically related to the necessity of a sufficiently vivid mixing in all models ($\tau_{\mathrm{mix}} \approx 10^6\,\mathrm{s}$).

The lower end of the cloud layer has a more complex structure. Phase equilibrium ($S = 1$) is achieved around 2000 K,

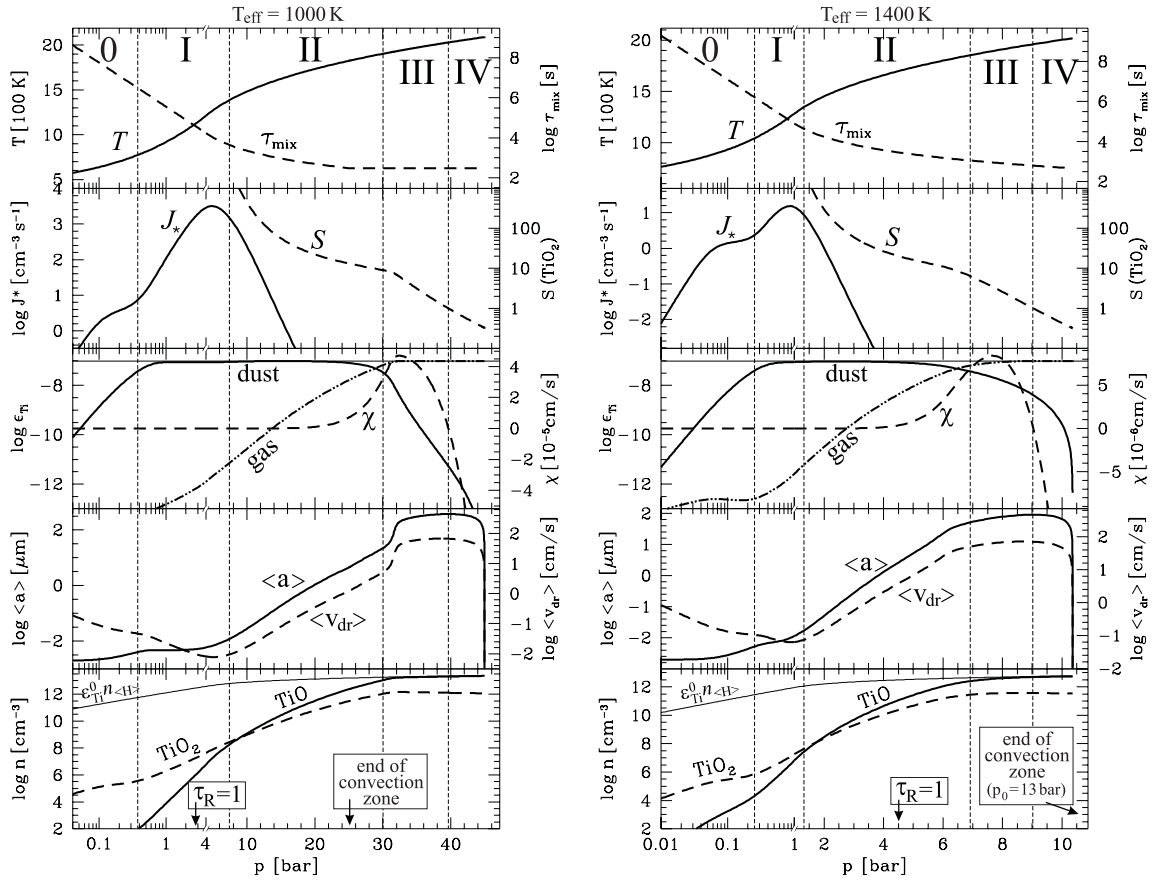

Fig. 2. Calculated TiO_2 cloud structures for models with $\log g = 5$ and different effective temperatures (l.h.s.: 1000 K – r.h.s.: 1400 K). Note the scaling of the partly logarithmic and partly linear p-axis. 1st panel: prescribed gas temperature T (solid), according to Tsuji (2002), and mixing time-scale $\tau_{\rm mix}$ (dashed). 2nd panel: nucleation rate $J_\star$ (solid) and supersaturation ratio $S_{\rm TiO_2}$ (dashed). 3rd panel: Ti abundance in the dust phase $\epsilon_{\rm Ti}^{\rm dust}$ (solid) and in the gas phase $\epsilon_{\rm Ti}$ (dashed-dotted). The solar value $\epsilon_{\rm Ti}^0$ is additionally indicated by a thin straight line. The dashed line shows the growth velocity $\chi_{\rm lKn}^{\rm net}$. 4th panel: mean particle size $\langle a\rangle = \sqrt[3]{3/(4\pi)}\,L_1/L_0$ (solid) and mean drift velocity $\langle v_{\rm dr}\rangle = \sqrt{\pi} g \rho_{\rm d} \langle a\rangle \,/\, (2\rho c_T)$ (dashed, see Eq. (66) in Paper II). 5th panel: molecular particle densities of TiO (solid) and TiO_2 (dashed). For comparison, the hypothetical total titanium nuclei density for solar abundances $n_{\langle \rm H\rangle}\epsilon_{\rm Ti}^0$ is depicted by a thin solid line. Parameters: $\tau_{\rm mix}^{\rm min} = 300$ s and $\beta = 2.2$.

hereafter called the *cloud base*. However, $\epsilon_{\rm Ti}^{\rm dust}$ already starts to deviate from $\epsilon_{\rm Ti}^0$ above the cloud base, when the dust particles have reached a certain critical size. We refer to this level, where again $f_{\rm cond}^{\rm Ti} = 1/e$, as the *rain edge* in the following. Interestingly, the cloud stretches even below its thermodynamically defined base[5], where the undersaturated gas is populated by evaporating grains which rain in from above.

According to our working definition (Eq. (16)), the *cloud layer* is featured by an almost maximum degree of condensation, $\epsilon_{\rm Ti}^{\rm dust} \lesssim \epsilon_{\rm Ti}^0$, and stretches from the cloud deck to the rain edge. In contrast, the amount of Ti left in the gas phase $\epsilon_{\rm Ti}$ depends strongly on the altitude above the rain edge. The gas becomes more and more depleted (metal-poor) with increasing altitude.

3.1. Structure of a quasi-static cloud layer

The vertical structure of the cloud layer results from a competition between the four relevant physical processes: mixing, nucleation, growth/evaporation and drift. Following the cloud structures inward (from the left to the right in Figs. 2 and 3), roughly five different regions can be distinguished, marked by the Roman digits, which are characterised by different leading processes concerning the dust component. The following physical characterisation is consistent with the classification outlined in Paper II.

0. Dust-poor depleted gas: High above the convection zone, the mixing time-scale is large and the elemental replenishment of the gas is too slow to allow for considerable amounts of dust to be present in the atmosphere. The few particles forming here are very small $\langle a\rangle < 10^{-2.5}\,\mu$m [6] and have drift velocities $\langle v_{\rm dr}\rangle \approx 1$ mm/s to 1 cm/s. These drift velocities, however, are sufficient to make the time-scale for gravitational settling $\tau_{\rm sink} = H_{\rm p}/v_{\rm dr}$ shorter than the mixing time-scale $\tau_{\rm mix}$, which causes these atmospheric layers to become dust-poor. The gas phase is strongly depleted in condensable elements. The Ti abundance in the gas phase $\epsilon_{\rm Ti}$ is reduced by a factor

[5] The size of this region may be overestimated because of the $J(V_\ell) \approx J_\star$ approximation, see Sect. 2.1.

[6] This size in fact corresponds to the parameter N_ℓ describing the minimum size of clusters regarded as "dust".

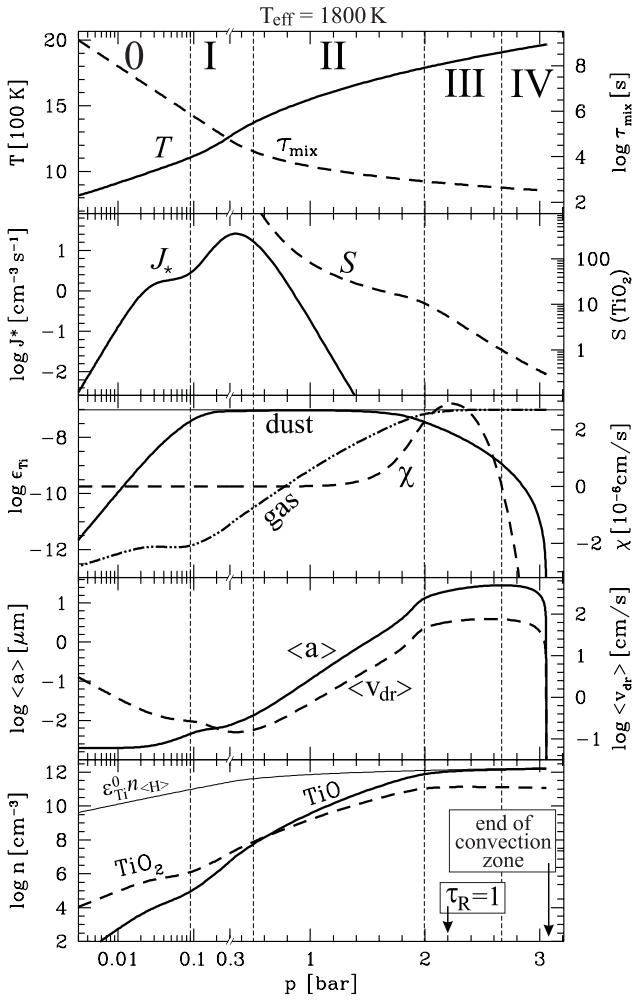

Fig. 3. Same as Fig. 2, but for $T_{\rm eff} = 1800$ K.

between 10^5 and 10^7 from its solar value. However, phase equilibrium ($S = 1$) is not achieved because even the very small disturbance of the atmosphere by mixing is sufficient to produce a solution which differs significantly from the trivial solution in the truly static case as discussed in Appendix A.

I. Region of efficient nucleation: Nucleation takes place mainly in the upper parts of the cloud layer, where the temperatures are sufficiently low and the elemental replenishment by mixing is sufficiently effective. Although the gas is strongly depleted in heavy elements in these layers, it is nevertheless highly supersaturated ($S > 1000$) such that homogeneous nucleation can take place efficiently[7]. Since very many seed particles are produced in this way, the dust grains remain small $\langle a\rangle < 0.01\,\mu$m and have small mean drift velocities $\langle v_{\rm dr}\rangle \approx 0.1$ mm s^{-1} ... 1 mm s^{-1}, which are even smaller than in region 0 because of the higher gas densities.

[7] To our surprise, the details of the applied nucleation theory have almost no effect on the resulting cloud structures. We have calculated test models with an arbitrarily modified value of the surface tension $\sigma^{\rm TiO_2} = 500\,{\rm erg/cm^2}$, which did not result in any noticeable changes. An explanation can be found via Eq. (8): As long as the total surface area of the dust particles ($\propto \rho L_2$) is negligible, the nucleation rate must equal $J_\star \approx n_{\langle {\rm H}\rangle}\epsilon_i^0/(\nu_{i,0}\, N_\ell\, \tau_{\rm mix})$, provided that $\epsilon_i \ll \epsilon_i^0$. Consequently, a change of $\sigma^{\rm TiO_2}$ results in a change of $\epsilon_{\rm Ti}$, but does not affect $J_\star$ significantly.

Table 1. Properties of the calculated TiO_2 cloud layers. The first three rows characterise the atmospheric gas stratification adopted from Tsuji (2002), the other quantities are obtained from our model calculations.

model for $T_{\rm eff}$ =	1000 K	1400 K	1800 K
$p\,(\tau_{\rm R} = 1)$	2.8 bar	4.5 bar	2.2 bar
Schwarzschild stability boundary p_0	25 bar	13 bar	3.2 bar
cloud layer [bar][1] (cloud deck – rain edge)	0.38–30	0.24–6.9	0.09–2.0
thermal stability of TiO_2 grains, i.e. $S = 1$ (cloud base)	2030 K (40 bar)	1975 K (9.4 bar)	1910 K (2.7 bar)
complete evaporation	45 bar	10.4 bar	3.1 bar
$\log \tau_{\rm mix}$ [s] at cloud deck	6.5	6.2	5.9
$\langle a\rangle$ at $\tau_{\rm R} = 1$	0.008 μm	3 μm	25 μm
$\langle a\rangle$ at rain edge	21 μm	51 μm	13 μm
$\langle a\rangle$ at cloud base	373 μm	91 μm	28 μm
$\max\{\langle \boldsymbol{v}_{\rm dr}\rangle\}$	68 cm s^{-1}	71 cm s^{-1}	76 cm s^{-1}
geometrical thickness of evap. region IV	900 m	1000 m	1100 m
Ti gas depletion factor at $\tau_{\rm R} = 1$	$10^{-5.2}$	$10^{-1.4}$	0.9

[1] Definition see Eq. (16).

II. Dust growth region: With the inward increasing temperature, the supersaturation ratio S decreases exponentially which leads to a drastic decrease of the nucleation rate $J_\star$ (see e.g. Eqs. (18) and (22) in Helling et al. 2001a). Consequently, nucleation becomes unimportant at some point, i.e. *the in situ formation of dust particles becomes inefficient in region II*. Here, the condensable elements mixed up by convective overshoot are mainly consumed by the growth of already existing particles, which have formed in region I and have drifted into region II. The gas is still strongly supersaturated $S \gg 1$, indicating that the growth process remains incomplete, i.e. the condensable elements provided by the mixing are not exhaustively consumed by growth. The dust component in region II is characterised by an almost constant degree of condensation ($\propto \epsilon_{\rm Ti}^{\rm dust} \propto L_3 \approx$ const.), while the mean particle size $\langle a\rangle$ and the mean drift velocity $\langle v_{\rm dr}\rangle$ increase inward. Consequently, the total number of dust particles per mass (L_0) and their total surface per mass ($\propto L_2$) decrease.

III. Drift dominated region: With the decreasing total surface of the dust particles ($\propto L_2$), the consumption of condensable elements from the gas phase via dust growth becomes less effective. At the same time, due to the increase of the mean particle size $\langle a\rangle$, the drift velocities increase. When the dust particles

have reached a certain critical size, $\langle a\rangle_{\rm cr} \approx 15\,\mu$m to $50\,\mu$m (see entry "$\langle a\rangle$ in cloud layer" in Table 1), the drift becomes more important than the growth, and the qualitative behaviour of the dust component changes. This happens at the borderline between region II and III, which we denote by rain edge. It is sometimes accompanied by a step-like increase of $\langle a\rangle$. The degree of condensation ($\propto\epsilon_{\rm Ti}^{\rm dust}$), and thereby the dust opacity, exponentially decreases inward in region III. We therefore expect that the optical appearance of the cloud layer possesses a relatively sharp lower edge at a particular altitude located in region III. Although the gas is still highly supersaturated $S \approx 1 \ldots 10$, the in situ formation of dust grains is ineffective as in region II. The depletion of the gas phase vanishes in region III, i.e. the gas abundances approach close-to-solar values. The grains reach their maximum radii at the lower boundary of region III (the cloud base): $\langle a\rangle \approx 30\,\mu$m to $400\,\mu$m at maximum drift velocities of about 70 cm/s, depending on $T_{\rm eff}$ (see Table 1). Since the residence time-scale of the settling grains is limited, the particles do not grow much further in region III, i.e. $\langle a\rangle$ increases slower than in region II.

IV. Evaporating grains: The gravitationally settling dust particles finally cross the cloud base and sink into the undersaturated gas situated below, where $S < 1$ and $\chi_{\rm lKn}^{\rm net} < 0$. Here, the dust grains raining in from above evaporate thermally. The evaporation of these dust particles, however, does not take place instantaneously, but produces a spatially extended evaporation region IV with a thickness of about 1 km. With decreasing altitude, the particles get smaller $\mathrm{d}\langle a\rangle/\mathrm{d}z < 0$ and slower $\mathrm{d}\langle v_{\rm dr}\rangle/\mathrm{d}z < 0$. Consequently, their residence times increase, and a run-away process sets in which finally produces a very steep decrease of the degree of condensation, terminated by the point where even the biggest particles have evaporated completely. We note that region IV, in particular, cannot be understood by stability arguments, but requires a kinetic treatment of the dust complex.

3.2. Influence of effective temperature

In general, the resulting cloud structures (Figs. 2 and 3) are similar for different values of the effective temperature, but their location with respect to the optical depth scale is different. For lower $T_{\rm eff}$, the active dust formation regions are situated deeper inside (note the different scaling of the p-axis) and the gas in the observable layers above the $\tau_{\rm R} = 1$ level becomes more metal-deficient. The latter result, an increasingly metal-poor gas for lower $T_{\rm eff}$, has been suggested as explanation for the disappearance of certain molecular features (like TiO and FeH) in the observed spectra of L dwarfs in comparison to M dwarfs (e.g. Leggett et al. 2001). We furthermore observe that the dust particles result to be larger for lower $T_{\rm eff}$: $\langle a\rangle_{\rm max} \approx 30\,\mu$m for $T_{\rm eff} = 1800$ K, $\langle a\rangle_{\rm max} \approx 400\,\mu$m for $T_{\rm eff} = 1000$ K. However, this tendency is reverse if the layer around $\tau_{\rm R} = 1$ is considered (see Table 1). The geometrical thickness Δz of the dust layer is found to increase slightly with decreasing $T_{\rm eff}$: $\Delta z \approx 3.1\,H_{\rm p}$ for $T_{\rm eff} = 1800$ K, $\Delta z \approx 4.4\,H_{\rm p}$ for $T_{\rm eff} = 1000$ K.

3.3. Influence of mixing

The models discussed in Sects. 3.1 and 3.2 reveal an important influence of the mixing by convective overshoot on the resulting properties of the dust particles and the cloud layers. Since the description of this mixing is very simple in this paper, and the determination of the mixing by convective overshoot, in general, is a matter of debate in the frame of 1D models, we will systematically study the influence of the two introduced parameters, $\tau_{\rm mix}^{\rm min}$ and β (see Eq. (9)), in this section.

Larger values for the minimum mixing timescale $\tau_{\rm mix}^{\rm min}$ simulate an overall less efficient mixing, which means a slower elemental replenishment of the atmosphere. An increase of $\tau_{\rm mix}^{\rm min}$, therefore, leads to reduced concentrations of TiO and TiO_2 molecules, in particular with regard to region II which is mainly responsible for the growth of the dust particles. Consequently, less matter condenses on the surface of the particles during their descent through the atmosphere, the particles remain smaller and obtain smaller drift velocities for larger $\tau_{\rm mix}^{\rm min}$.

These altered particle properties result in considerable structural changes. Figure 4 demonstrates that, if $\tau_{\rm mix}^{\rm min}$ is increased from 300 s to 2000 s (l.h.s.), the resulting cloud layer starts to adjust to a qualitatively different structure, now characterised by the regions I′ to IV′:

1) The nucleation region I′ is now situated *above* the cloud layer as defined by Eq. (16)[8].
2) The drift velocities of the smaller particles remain subcritical, which does not allow for the occurrence of a drift dominated region III as in the $\tau_{\rm mix}^{\rm min} = 300$ s – models. Instead, a new region III′ develops which is characterised by an almost saturated gas ($S \gtrsim 1$), indicating that the growth becomes exhaustive in region III′. A *self-regulation mechanism* takes control which approximately installs phase equilibrium around the cloud base (regions III′ and IV′).
3) The dust layer physically now stretches even below the thermodynamically defined cloud base. Together with point (1), this causes the cloud layer to be situated deeper in the atmosphere.
4) If $\tau_{\rm mix}^{\rm min}$ is increased to 10^7 s (r.h.s. of Fig. 4), full condensation is not achieved anywhere in the atmosphere, and the dust layer virtually disappears. The solution finally becomes similar to the trivial solution discussed in Appendix A, namely a saturated gas ($S \to 1$) without dust ($\epsilon_{\rm Ti}^{\rm dust} \to 0$) for $\tau_{\rm mix}^{\rm min} \to \infty$.

The Ti gas abundance $\epsilon_{\rm Ti}$ in fact crosses the $\epsilon_{\rm Ti}^0$-line at the cloud base (barely visible in Figs. 2 and 3). *The release of condensable matter from the surface of the evaporating grains enriches the gas below the cloud base with heavy elements* $\epsilon_{\rm Ti} > \epsilon_{\rm Ti}^0$ in region IV/IV′. If $\tau_{\rm mix}$ is sufficiently large, as assumed in Fig. 4, this enrichment leads to a noticeable increase of the supersaturation ratio $S\nearrow 1$ in region IV′. For more vivid mixing, as assumed in Figs. 2 and 3, the enrichment is "mixed away" in region IV.

[8] In fact, in the $\tau_{\rm mix}^{\rm min} = 300$ s – models, the nucleation region I is always a part of the cloud layer.

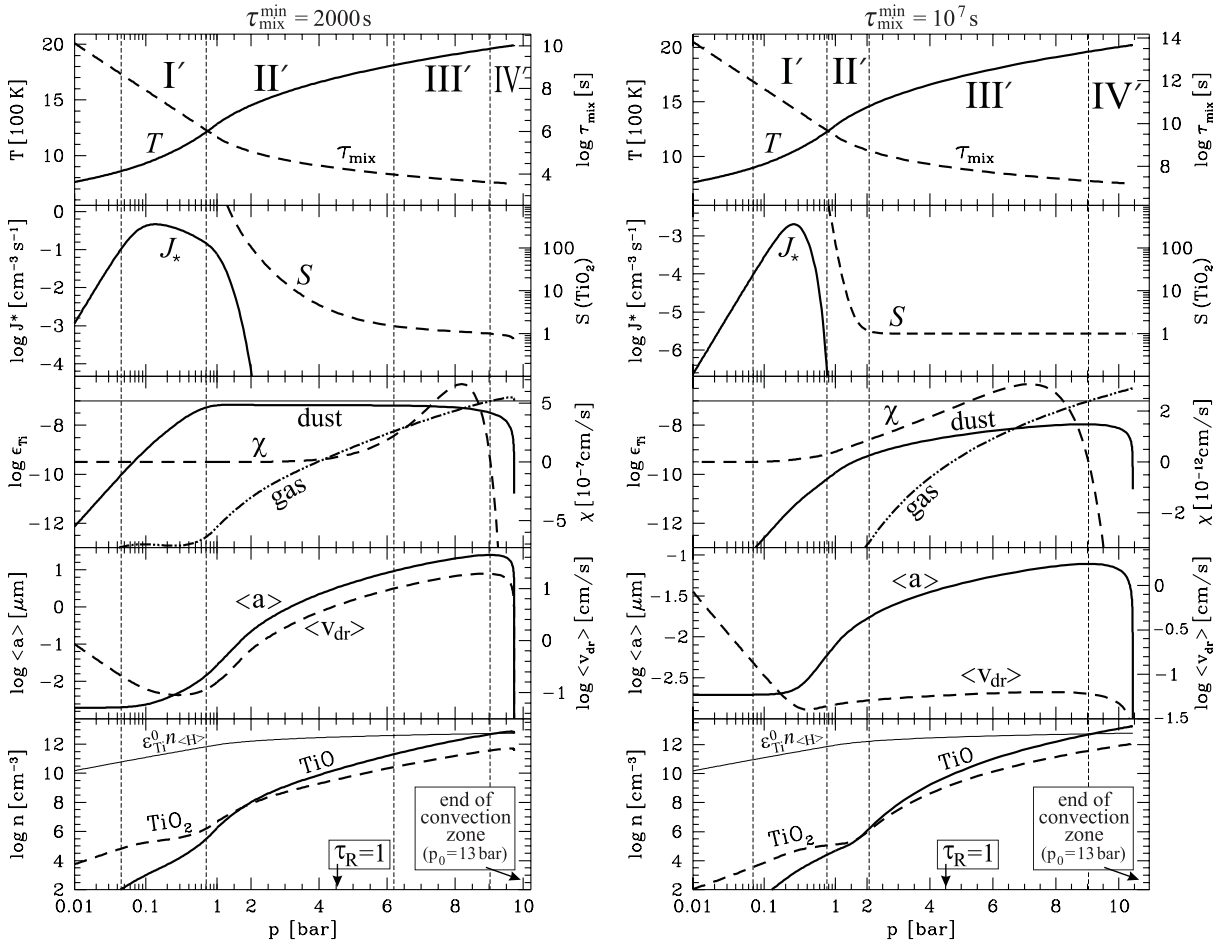

Fig. 4. Same as Fig. 2, but for two enlarged values of the minimum mixing timescale $\tau_{\rm mix}^{\rm min}$ (see Eq. (9)), as indicated by the top labels. Other parameters: $T_{\rm eff} = 1400$ K and $\beta = 2.2$.

The models depicted in Figs. 2, 3 and on the l.h.s. of Fig. 4 are featured by an almost constant, maximum value of $\epsilon_{\rm Ti}^{\rm dust}$ in the cloud layer, which results to be approximately equal to the Ti abundance in the gas being mixed up (here $\epsilon_{\rm Ti}^0$). This is a natural result of an undisturbed, complete condensation process. Evidently, the disturbance of the dust formation by rain-out and mixing is usually small in our models, in agreement with the time-scale discussion of Paper II, where it was shown that the drift motion of dust grains in brown dwarf atmospheres usually operates on much longer time-scales than nucleation and growth.

However, if the elemental replenishment by convective mixing becomes too ineffective, $\epsilon_{\rm Ti}^{\rm dust}$ does not reach $\epsilon_{\rm Ti}^0$ anymore (see r.h.s. of Fig. 4), the cloud layer disappears and the atmosphere becomes apparently dust-free. Figure 5 shows that the maximum value of $\epsilon_{\rm Ti}^{\rm dust}$ achieved in the atmosphere starts to deviate from $\epsilon_{\rm Ti}^0$ around $\tau_{\rm mix}^{\rm min} \approx 10^6$ s. In this case, the loss of condensable elements from a fully condensed gas via rain-out is larger than the gain of condensable elements by mixing, even if the dust particles are very small.

Figure 6 demonstrates the influence of the logarithmic slope β, the second parameter introduced to describe the mixing by convective overshoot. An enlargement of this parameter simulates a steeper increase of $\tau_{\rm mix}$ with increasing height above the convectively unstable zone. The main effect of an increase of β is a narrowing of the cloud layer, but the existence of the cloud layer is not affected. Noteworthy, the value of $\log \tau_{\rm mix}$ at the cloud deck is relatively constant, ranging in 5.5 to 6.3 for all models with $T_{\rm eff} = 1400$ K, $\tau_{\rm mix}^{\rm min} = 300$ s and varying β (compare also Table 1). We conclude that all layers of brown dwarf atmospheres that are cool enough to ensure the thermodynamical stability of dust grains should in fact be dusty as long as the convective mixing time-scale $\tau_{\rm mix}$ is shorter than about 10^6 s ≈ 10 days[9].

4. Discussion and outlook

4.1. Validity of the Kn ≫ 1 approximation

In this paper, we have focused on the Kn ≫ 1 case, which enabled us to use an unique system of dust moment equations throughout the atmosphere[10]. However, Fig. 7 shows that the Knudsen numbers may actually fall short of unity in the deeper layers, e.g. below $p \approx 3$ bar in the $T_{\rm eff} = 1400$ K-model which approximately coincides with the $\tau_{\rm R} = 1$–level. This means

[9] Except for the drift dominated region III (if present), see Sect. 3.1.

[10] A different system of dust moment equations for the opposite case Kn ≪ 1 has been derived in Paper II.

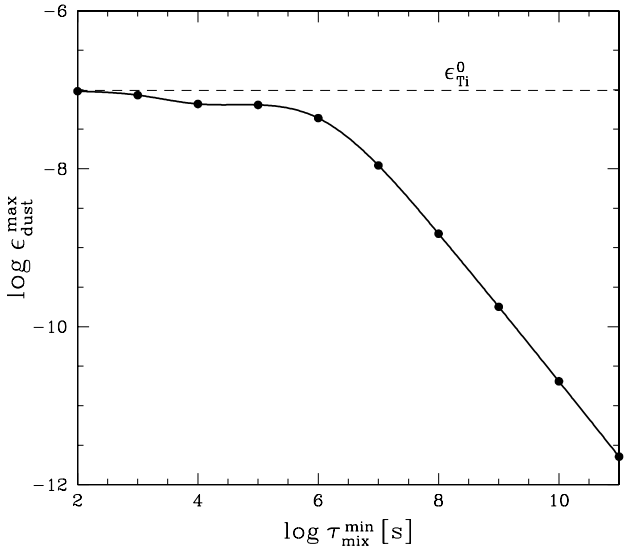

Fig. 5. Maximum of the Ti abundance in the solid phase $\epsilon^{\rm max}_{\rm dust} = \max_z\{\rho(z)L_3(z)/(n_{\langle \rm H\rangle}(z)\Delta V_{\rm TiO_2})\}$ as function of the minimum mixing time-scale $\tau^{\rm min}_{\rm mix}$. The circles indicate the calculated models for $T_{\rm eff}$ = 1400 K and β = 2.2. In comparison, the solar titanium abundance $\epsilon^0_{\rm Ti}$ is shown as dashed line.

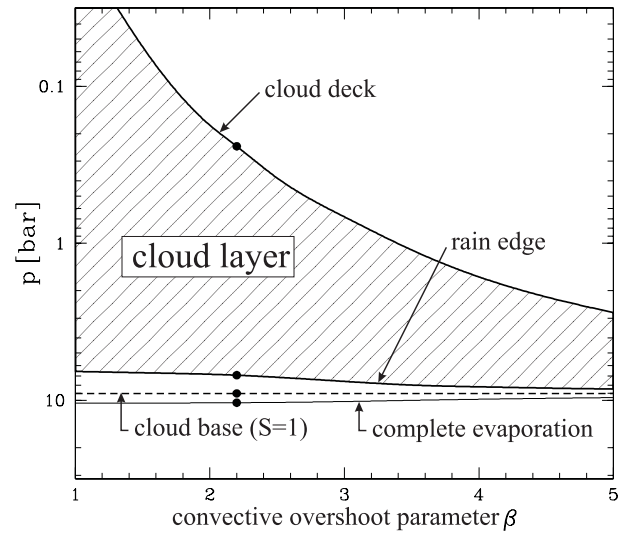

Fig. 6. Location of the cloud layer as function of convective overshoot parameter β (see Eq. (9)) for $T_{\rm eff}$ = 1400 K and $\tau^{\rm min}_{\rm mix}$ = 300 s. The full circles denote the model with β = 2.2 depicted in detail on the r.h.s. of Fig. 2.

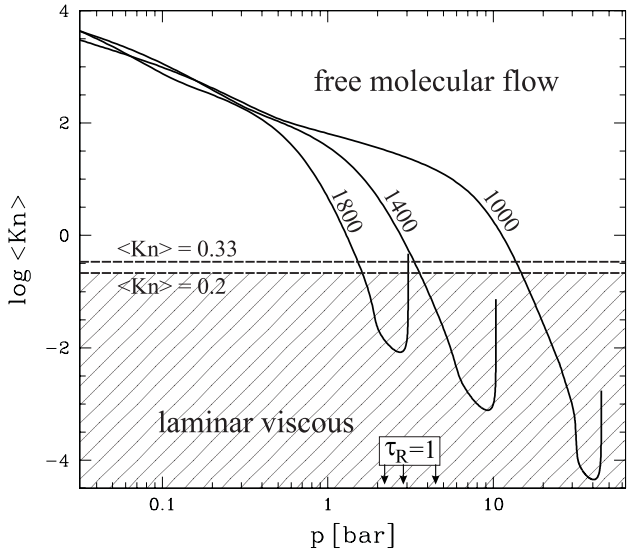

Fig. 7. Mean Knudsen number of the dust component, derived from $\langle a\rangle$, as function of the gas pressure for the $T_{\rm eff}$ = 1000 K, 1400 K and 1800 K models. The small arrows at the bottom indicate the atmospheric layers where the Rosseland optical depths approaches unity. The dashed lines indicate the critical Knudsen numbers for friction and growth, respectively (compare Paper II).

that the mean free path of a gas particle becomes smaller than a typical grain diameter. The physical description of the growth and the frictional force are different in this case, i.e. our model can only provide a possibly quite rough picture from these layers. Here, the true drift velocities are probably larger and the true growth velocities are probably smaller as compared to our results, i.e. we expect that $\langle a\rangle$ remains smaller in the deeper layers as compared to Figs. 2 and 3.

However, Fig. 7 also demonstrates that the higher atmospheric layers can very well be treated in the Kn $\gg$ 1 limiting case. Since the problem is formulated in terms of first order differential equations which are integrated inward, the solution in the outer regions does not depend on the uncertainties concerning the deeper layers. Therefore, we conclude that our results are appropriate for the upper layers, approximately down to the $\tau_{\rm R}$ = 1 level, which are most interesting from an observational point of view. This restriction is more critical for models with larger $T_{\rm eff}$.

A more realistic description of the deeper layers could be achieved by performing a Knudsen number fall differentiation with respect to $\langle$Kn$\rangle$, i.e. to start with the Kn $\gg$ 1 moment equations in the outer layers as outlined in this paper, but then to switch to the Kn $\ll$ 1 moment equations (see Paper II) as soon as $\langle$Kn$\rangle$ has dropped below a certain critical value, e.g. 0.3. However, such a procedure is problematic anyway, since all dust particles in the size distribution function would be treated in the same Knudsen number limiting case. A more profound solution would require the integration over the size distribution, which could approximately be determined from the calculated dust moments (see Sect. 6.5 in Paper II).

4.2. Convective mixing

The results presented in Sect. 3 have been obtained by assuming a depth-dependent replenishment of the atmosphere with dust-free gas of solar abundances (from the deep interior of the brown dwarf) on a prescribed time-scale $\tau_{\rm mix}(z)$. Although this approach is certainly a poor description of the true convective mixing occurring in these atmospheres, it has allowed for a first detailed study of the cloud structures in brown dwarf atmospheres, simple enough to investigate the influence of the convective mixing on the dust formation in a systematic way.

However, considering a convectively ascending bubble of gas from the deep interior, which is dust-free at first, the temperature/density conditions will change gradually in this

element. Hence, the key process of nucleation and the dust growth can already occur during the ascent of this element, i.e. well before the element has reached the upper atmospheric layers, where it finally disperses in the surrounding gas.

Therefore, a quasi-diffusive approach for the mixing may be more appropriate[11]. In this case, the local net gain of species k can be quantified by $-\nabla \boldsymbol{j}_k^{\rm mix}$ where the mean convective flux of species k is given by

$$\boldsymbol{j}_k^{\rm mix} = -\, D_{\rm mix}\, \rho \nabla c_k. \qquad (17)$$

c_k is the mass concentration of species k and $D_{\rm mix}(z)$ the diffusion constant for convective mixing, which can be adapted to the results obtained from a convection theory, e.g. mixing length theory or the theory developed by Kuhfuß (1987), see e.g. Wuchterl & Tscharnuter (2003). The determination of $D_{\rm mix}$ for radiative layers (mixing by convective overshooting) is discussed by Freytag et al. (1996). Adopting this approach to our problem, the mixing terms $\nabla\cdot\left(D_{\rm mix}\,\rho\nabla L_j\right)$ and $\nabla\cdot(D_{\rm mix}\, n_{\langle\rm H\rangle}\nabla\epsilon_i)$ could be used instead of $-\rho L_j/\tau_{\rm mix}$ and $n_{\langle\rm H\rangle}(\epsilon_i^0-\epsilon_i)/\tau_{\rm mix}$ in Eqs. (7) and (8), respectively. In that case, the equation system to be solved becomes a system of second order partial differential equations with the need to specify inner and outer boundary conditions, a problem which requires a more careful numerical treatment.

In return, the dust formation may also have an important influence on the convection, e.g. via the release of the heat of condensation during the grain growth process or via opacity effects. For example, Helling et al. (2001a) have shown that the increase of the opacity due to dust formation will cause a transition from an almost adiabatic to an almost isothermal behaviour of the dust/gas mixture. Thus, a consistent treatment of convection and dust formation is required to come to more definite conclusions.

However, one-dimensional approaches for the convection can only provide a rough description of the underlying hydrodynamical processes by considering temporal and spatial averages. A more direct approach was a 3D dynamical simulation, where a description of the large-scale mixing becomes obsolete. We want to emphasise, however, that even in such models (e.g. LARGE EDDY SIMULATIONS) the true mixing down to the Kolmogoroff-scale requires a sub-grid modelling, because the smaller scales cannot be resolved on the typically large-scale computational grids (see e.g. Menevean & Katz 2000; Pijpers & Habing 1989). Furthermore, structure formation processes are often seeded in the small scale regime, as e.g. known from combustion engineering.

4.3. Spectral appearance of cloud layers

The calculation of optical depths across the cloud layers provides a simple estimate for the influence of the dust on the spectral appearance of brown dwarfs. For consistency reasons, we will at first consider the TiO_2 cloud layers as resulting from our model, before we will comment on this topic in a more general way.

Table 2. Optical depths of the calculated TiO_2 cloud layers.

$T_{\rm eff}$	1000 K	1400 K	1800 K
$\Delta\tau_{\rm Ross}$	1.6×10^{-3}	3.5×10^{-4}	1.0×10^{-4}
$\Delta\tau_{\rm Pl}$	8.1×10^{-2}	1.6×10^{-2}	4.9×10^{-3}
$\Delta\tau_{1.25\ \mu\rm m}$	1.3×10^{-3}	3.1×10^{-4}	9.0×10^{-5}
$\Delta\tau_{2.2\ \mu\rm m}$	1.4×10^{-3}	3.2×10^{-4}	9.4×10^{-5}
$\Delta\tau_{13.3\ \mu\rm m}$	19	4.3	1.3

In the small particle limit (SPL) of Mie theory[12], the total extinction coefficient of the dust particles can be determined from

$$\kappa_{\lambda,\rm ext}^{\rm dust} = \frac{3}{4}\, Q'(\lambda)\, \rho L_3, \qquad (18)$$

because the scaled extinction efficiency $Q'(\lambda) = Q_{\rm ext}(a,\lambda)/a$ becomes size-independent (Gail et al. 1984). Appendix B provides fit-formulae for the Planck and Rosseland mean, $Q'_{\rm Pl}(T)$ and $Q'_{\rm Ross}(T)$, as calculated from the optical constants of rutile (Th. Posch 1999, priv. comm.). The increase of e.g. the Rosseland mean optical depth $\tau_{\rm Ross}$ across the cloud layer is

$$\Delta\tau_{\rm Ross} = \int \frac{3}{4}\, Q'_{\rm Ross}(T)\, \rho L_3\, {\rm d}z. \qquad (19)$$

The calculated values of $\Delta\tau$ (Rosseland mean, Planck mean and monochromatic) are listed in Table 2.

These results show that the calculated TiO_2 cloud layers are *basically optically thin* and should have no important direct influence on the spectra in the optical and near IR spectral region. This is a consequence of both the low Ti abundance and, in particular, the glassy character of the crystalline TiO_2 extinction. These grains are transparent in the optical and near IR whereas they are opaque around 10 μm−30 μm (see Fig. 2 in Woitke 1999). Thus, optical and near IR spectroscopy can probably neither confirm nor exclude the existence of glassy, crystalline grains like TiO_2 in the photospheres of brown dwarfs. Direct observational evidence for such grains is rather achievable by mid IR spectroscopy, where the main vibrational modes of the solid lattice structure are situated and where characteristic dust absorption features can be expected.

Nevertheless, the formation of solid TiO_2 can be expected to have an important indirect influence on the spectra via the consumption of molecular absorbers, here in particular TiO. Table 1 (last row) shows how the photospheric layers with $\tau_{\rm Ross} < 1$ become increasingly Ti-depleted with decreasing $T_{\rm eff}$, which should result in a vanishing of the TiO-bands and could possibly cause a bluening of the spectra with decreasing $T_{\rm eff}$ as observed.

However, TiO_2 is only an example species chosen for practical reasons according to the purpose of this paper (see Sect. 2.2). If the resulting dust structures for TiO_2 are simply

[11] We note, however, that the character of the convective mixing can, at least partly, also be large-scale, i.e. it seems possible that an uncondensed bubble of gas from the interior reaches upper layers and disperses before it cools and condenses, where our simple ansatz with $\tau_{\rm mix}$ seems appropriate.

[12] Larger but fewer dust particles (at constant dust mass) generally produce *smaller* total dust opacities.

scaled up to certain types of silicates which are opaque in the near IR (e.g. iron containing grains like $MgFeSiO_4$ with 2–3 orders of magnitude higher extinction efficiencies in the near IR, assuming SPL) and have potentially 2.5 orders of magnitude higher abundance, the silicate cloud layers were optically thick throughout substantial parts of the photosphere. This generalisation is possibly in conflict with current semi-empirical models of T dwarfs (e.g. Allard et al. 2001; Tsuji 2002) which predict geometrically thin dust layers.

This apparent discrepancy between our model and current semi-empirical models in case of T dwarfs may be caused by several factors. Various assumptions in our model may need to be revisited, in particular the description of the chemical and physical processes involved in the dust formation, but also the treatment of the convective mixing and the missing consistency between dust formation, turbulence, convection and radiative transfer. Last but not least, already the assumption of a 1D static atmosphere may be questionable and may enforce a best-fitting solution which is not in agreement with current dust formation theory (e.g. a thin dust layer instead of an extended but clumpy dust distribution). More elaborate, maybe multi-dimensional models must be developed to investigate this point further, where detailed comparisons to observations are essential to improve the models.

4.4. Comparison to other models

According to our present knowledge, we have presented the first model calculations for brown dwarf atmospheres where the coupled problem of dust formation, precipitation and element consumption has been solved on the basis of a kinetic description of the underlying physical and chemical processes. A consistent incorporation of this description into classical stellar atmosphere models (to account for the important feedbacks of the dust on the atmospheric structure via radiative transfer effects and the convection) has not yet been performed.

So far, other works have mainly focused on the consequences of the presence of dust on the spectral appearance of brown dwarfs, thereby treating the dust complex in a much more simplified way. These approaches have in common that the possible existence and the properties of the dust particles are completely deduced from *local arguments and considerations*. A possible connection between the site of formation (nucleation) of a dust grain and its occurrence in another place (via winds or gravitational settling) has not been considered in any other model.

Allard et al. (2001) have relied on the assumption of chemical and phase equilibrium between the molecules in the gas and a huge collection of solid and liquid materials. If a solid material is found to be thermodynamically stable, the respective elements are depleted from the gas phase down to the $S = 1-$ level and the amount of dust present in the atmosphere is either given by element conservation constraints (the case of complete condensation) or is assumed to be zero (the case of complete gravitational settling, see also Burrows & Sharp 1999). Each condensate is assumed to be present in form of homogeneous spherical particles, i.e. no dirty or core-mantle grains. The size distribution known from the interstellar medium is utilised.

According to our model, phase equilibrium ($S = 1$) is strictly valid only at the cloud base (by definition). All other regions are in phase non-equilibrium because of incomplete growth or evaporation. However, the self-regulation mechanism characteristic for region III′ (see Sect. 3.3) can lead to a considerably extended, approximately saturated layer ($S \approx 1$) around the cloud base. Thus, the assumption of phase equilibrium may in fact be reasonable in certain parts of the atmosphere. The location and thickness of this region, however, depends on the condensate and, in particular, on the strength of the convective mixing. The mixing by convective overshoot as adopted from Ludwig et al. (2002) results to be too vivid in all layers to allow for the occurrence of a $S \approx 1-$region. Only if this mixing is artificially reduced by a factor $\sim$10, an extended region with approximate phase equilibrium appears.

Tsuji (2002) has suggested that condensates in cool dwarf atmospheres are present in form of layers with strict inner and outer boundaries. The inner boundary, associated with a certain temperature denoted by $T_{\rm cond}$, is related to the thermodynamical stability of the dust particles in the surrounding gas of solar abundances. The upper boundary, parameterised by $T_{\rm cr}$, is related to the assumption, that the dust particles must remain extremely small (of the order of the critical cluster size $a_{\rm cr}$), because they would grow too large and start to settle gravitationally otherwise. For $T_{\rm cond} > T > T_{\rm cr}$, the particles are assumed to be constantly forming and re-evaporating, thereby circumventing the problem of the gravitational settling.

Our results confirm that the dust is mainly present in form of a layer and that the lower boundary of this layer is related to the thermodynamical stability of the dust particles. However, our model suggests a different physical explanation for the upper boundary. According to our results, the (smooth) cloud deck is related to the requirement of a sufficient elemental replenishment by convective mixing. Already a very slow mixing of the atmosphere (characteristic time-scale $\tau_{\rm mix} \approx 10^6$ s) can maintain an ongoing cycle of nucleation $\rightarrow$ growth $\rightarrow$ precipitation $\rightarrow$ evaporation $\rightarrow$ mixing. Therefore, we think that there is no need to circumvent the dust precipitation. Convective overshoot can easily provide such a mixing activity even a few scale heights above the convectively unstable layers.

We also disagree with the chemical argumentation of Tsuji (2002), because the critical cluster corresponds to an *unstable* equilibrium (the critical cluster is the most unstable cluster on the most efficient chemical pathway to dust, see e.g. Feder et al. 1966). It will be difficult to maintain a system like a brown dwarf atmosphere in such a fine-tuned unstable equilibrium state. According to our results, the upper atmospheric regions in fact contain many very small dust particles, but the size of these particles is a kinetic consequence of the large nucleation rates in these layers and cannot be deduced from stability arguments.

Cooper et al. (2003) utilise the chemical and phase equilibrium code of Burrows & Sharp (1999) to determine whether dust particles of a certain kind are thermodynamically stable in a solar composition gas. If stability is assured, the mean size of the particles is deduced from local time-scale arguments based on Rossow (1978), considering growth, coagulation (partly denoted by coalescence), precipitation and convective mixing. The amount of dust is prescribed by introducing a free parameter $S_{\max} \approx 0.01$, the so-called maximum supersaturation. Thereby, the supersaturation ratio of the gas (denoted by S in our paper) is fixed throughout the atmosphere and the mass of dust present in the atmosphere scales with the saturation vapour pressure $p_{\rm sat}(T)$, which decreases exponentially with decreasing temperature. Consequently, the vertical structure of the dust also results to be a layer with a strict lower boundary and an exponentially decreasing dust-to-gas ratio above the cloud base.

Noteworthy, Cooper et al. (2003) derive "modal" particle sizes ($5\,\mu$m$\ldots 300\,\mu$m) that are comparable to our maximum values of $\langle a \rangle$, although the physical description, e.g. of the dust growth, is very different. We find, however, that the mean size of the dust particles $\langle a \rangle$ is often much smaller than the maximum particle size $a_{\max}$ as derived from local time-scale arguments (see Paper II), in particular regarding the upper atmospheric layers. Therefore, we think that local time-scale arguments are not sufficient – the problem requires a kinetic treatment. We furthermore remark that, in contrast to Cooper et al. (2003), our results suggest that the supersaturation ratio S varies strongly with altitude, in particular regarding the higher atmospheric layers. The supersaturation ratio S is strongly affected by the convective mixing.

In the Cooper et al. model, the "modal" particle size is a function of depth and condensate. The largest particles occur at the cloud base, which is in agreement with our results. Sengupta & Krishan (2001) have suggested that polarisation measurements provide a possibility to deduce the mean size of dust particles in brown dwarf atmospheres. The degree of polarisation increases strongly with increasing particle size and multiple scattering can even amplify this effect. According to Sengupta (2003), the observed degree of polarisation of the brown dwarf DENIS-P J0255–4700 ($T_{\rm eff} \approx 1400\,$K, $\log g \approx 5$) suggests particle radii of about $5\,\mu$m, if single scattering of spherical particles is considered. This lies well in the range of mean sizes derived from our model for $T_{\rm eff} = 1400\,$K in the layers around $\tau_{\rm R} = 1$ (see r.h.s. of Fig. 2).

Helling et al. (2001a) have studied the onset of the dust formation process in small ascending convective gas elements under turbulent conditions typical for brown dwarf atmospheres. The same physical description of nucleation and dust growth is applied as in this paper, except for the evaporation and the particle drift which have been neglected. The convection is assumed to energise turbulence, which creates a strongly varying velocity field and fluctuations of all thermodynamical quantities on various length scales, down to the Kolmogoroff-scale ($\eta \approx 10^{-2}\,$cm). Acoustic waves are shown to be capable to initiate the dust formation process via nucleation events caused by the superposition of two or more expansion waves, even in layers which are usually too hot for nucleation. The refractory elements in the gas phase soon condense on the surface of these first seed particles. When a considerable fraction of the condensable elements is consumed, the increasing dust opacity reinforces radiative cooling and causes the thermodynamical behaviour of the gas-dust-mixture to change from almost adiabatic to almost isothermal (fast radiative relaxation), which in return might affect the convective stability of the atmosphere. The dust component results to be spatially very inhomogeneous.

We want to clarify that the effect of *turbulent small-scale fluctuations* on the dust formation has been neglected in the current paper – although it may be important. The aim of this paper is to understand the *large-scale structure* of a cloud layer in brown dwarf atmospheres. Accordingly, we have developed a model for the largest scales where the small-scale processes can principally not be resolved. In order to include such effects approximately, appropriate sub-grid closure terms for the dust moment equations must be developed.

5. Summary and conclusions

In this paper, first model calculations for cloud layers in quasi-static brown dwarf atmospheres have been presented which are based on a kinetic description of the underlying microphysical and chemical processes: nucleation, growth, evaporation, element depletion, sedimentation and mixing. We have used a system of differential equations for the moments of the dust size distribution function, which has been developed in Paper II, in the stationary case for large Knudsen numbers. The consumption of condensable elements is an essential part of this description and, therefore, the depletion of the gas phase from condensable elements is a consistent part of the results. The model calculations are restricted to one exemplary refractory dust species (TiO_2) which is enough to study the control mechanisms for the dust formation and the general structure of cloud layers in brown dwarf atmospheres.

According to our model, an ongoing cycle of nucleation → growth → precipitation → evaporation characterises the large-scale structure of a cloud layer, related to the life cycle of dust grains in brown dwarf atmospheres. This cycle is maintained by convective mixing. Without mixing, all dust particles would settle gravitationally, leaving behind a saturated (i.e. strongly metal-deficient) dust-free atmosphere above the cloud base. However, cool dwarf stars (M, L, T) are almost fully convective, which leads to a replenishment of the atmosphere with condensable elements from the deep interior of the star. This convective mixing is extended into the upper, radiative parts of the atmosphere via overshooting, which results to be sufficient to initiate the dust formation process even a few scale heights above the convectively unstable zone. Thus, the convection triggers the formation and resultant properties of the emergent dust particles.

The vertical structure of the atmospheric dust stratification is found to be an almost fully condensed layer with smooth boundaries. The upper boundary (cloud deck) is related to the requirement of a minimum mixing activity (mixing time-scale $\tau_{\rm mix} \approx 10^6\,$s). The location of this cloud deck depends on the

assumptions about the decrease of the mixing efficiency by convective overshoot with increasing height above the convectively unstable zone. The lower boundary (cloud base) is mainly determined by the thermodynamical stability of the grains ($S = 1$). However, if the mean size of the dust particles exceeds a certain critical value in the cloud layer (15 μm to 50 μm), the particles start to rain out efficiently. This occurs below a certain level in the atmosphere (rain edge) which is usually located above the thermodynamically defined cloud base. The rain-out leads to a dynamic dilution of the dust component, i.e. a considerable decrease of the dust-to-gas ratio below the rain edge.

Five different regions can be distinguished, ordered by the leading physical process for the dust component, which correspond to a particular height in a quasi-static model:

0) The uppermost parts of the atmosphere are strongly depleted (metal-poor) and almost dust-free, because the elemental replenishment by convective overshoot is insufficient.

I) *Nucleation:* The formation of seed particles mainly occurs around the cloud deck where the gas is cool enough (e.g. $T \approx 1000$ K to 1400 K for TiO_2) and the elemental replenishment is sufficiently effective. As a result, the gas is strongly depleted (metal-poor), but nevertheless highly supersaturated[13].

II) *Growth:* The particles formed in region I drift into the warmer regions below, where the in situ formation (nucleation) is ineffective. The particles grow substantially in this layer, thereby consuming the condensable elements which are constantly replenished by the convective mixing. However, the growth process remains incomplete, i.e. the gas is still highly supersaturated.

III) *Drift:* With increasing particle size, the drift motion becomes the leading physical process below a certain atmospheric level (rain edge). The dust particles mainly drift through the region below the rain edge without much further growth. Maximum sizes between 30 μm and 400 μm are reached and the depletion of the gas phase, being still supersaturated, vanishes.

IV) *Evaporation:* The dust particles finally cross the cloud base (defined by $S = 1$, here at $T \approx 2000$ K for TiO_2) and populate the undersaturated gas below, down to the point where the dust particles shrink, decelerate and vanish. The evaporation of these dust particles can create a metal-enriched region below the cloud base.

This stratification cannot be understood by stability arguments, but requires a kinetic treatment of the dust complex. According to our results, the atmosphere is generally in phase-non-equilibrium ($S \neq 1$), except for the cloud base, where the element abundances coincide with those of the uncondensed gas being mixed up. Consequently, the application of numerical codes which assume chemical and phase equilibrium, simply including liquid and solid phases as additional specimen, seems questionable. However, a self-regulation mechanism exists for artificially reduced mixing which leads to the formation of a restricted layer around the cloud base where phase equilibrium is approximately valid ($S \approx 1$). The existence, location and spatial extension of this layer depends on the material, the stellar parameters and, in particular, on the convective mixing.

From an observational point of view, it is important to note that the gas becomes more and more depleted in the upper atmosphere. The maximum degree of depletion of Ti with respect to the cloud base results to be 5 to 7 orders of magnitude in our model, reached in the upper atmospheric layers, which are mainly responsible for the observational molecular features. The degree of gas depletion decreases inward down to the rain edge, where the Ti element abundance reaches its solar values.

The mean particle size $\langle a \rangle$ is generally found to decrease by several orders of magnitude from a maximum value present at the cloud base with increasing height. This maximum size ranges in 30 μm to 400 μm, which is consistent with the quantity $a_{\max}$ defined in Paper II. However, the particles generally remain much smaller than $a_{\max}$ high above the cloud base and/or in case of weak convective mixing.

A lower effective temperature $T_{\rm eff}$ of the brown dwarf mainly results in a shift of the active dust formation zone into deeper layers. The basic structure of the cloud layer and the resultant properties of the dust particles remain similar with respect to the cloud base. However, if only the results at $\tau_{\rm R} = 1$ are considered, the properties of the cloud layer depend strongly on $T_{\rm eff}$. In particular, the dust particles are much smaller (but more numerous) and the gas is more depleted for lower $T_{\rm eff}$ at the $\tau_{\rm R} = 1$ – level.

Generally speaking, the formation of solid particles and fluid droplets in the atmospheres of very cool dwarfs unfolds a gap in the current status of standard stellar atmosphere theory. A kinetic description of nucleation, net growth, element depletion and sedimentation of the dust particles by means of differential equations seems capable to fill this gap. *Local arguments and considerations*, which have been mainly used so far, *are not sufficient* because they cannot account for the spatial (and temporal) coupling between the different atmospheric layers due to the drift motion of the particles. A more physical description of the formation and gravitational settling of dust particles seems likely to provide a better understanding of the spectral appearance and the evolutionary sequence from cool M-dwarfs over L-dwarfs to T-dwarfs.

Beside an extension of our preliminary models to more than one dust species (which involves the problem of core-mantle and possibly dirty grains), the development of turbulent closure terms for small-scale fluctuations and a more general treatment of small and large Knudsen numbers, the remaining uncertainties of our model are mainly introduced by the current treatment of convective mixing. A fine-tuned

[13] It is important to note that the formation of high-temperature condensates (with sublimation temperatures of the order of 2000 K) requires to overcome the nucleation barrier. The pre-existence of some seed particles in the condensing gas of another unidentified kind (in analogy to the aerosols in the Earth atmosphere) seems questionable here, because the temperature difference nucleation-stability (here 600 K to 1000 K) is large compared to the difference of the sublimation temperatures among the different high-temperature condensates.

counterbalance between the *upward directed flux of condensable elements via convection* and the *downward transport of condensable elements via the formation, gravitational settling and thermal evaporation of dust grains* is responsible for the vertical structure of refractory elements in the atmosphere. Moreover, since the dust formation may even have an important feedback on the convection itself (via the release of the latent heat of condensation and via opacity effects), a simultaneous treatment of convection and dust formation, consistently coupled to a frequency-dependent radiative transfer, is required for more realistic models of brown dwarf atmospheres.

Acknowledgements. We thank Takashi Tsuji for providing numerical versions of his brown dwarf model structures and Hans-Günter Ludwig for his remarks about the convective mixing. We are grateful to Coryn Bailer-Jones for commenting on our results, and Waltraud Woitke for taking care of Johanna, thereby enabling us to continue this work. We acknowledge the financial supported by the *DFG* (grand SE 420/19-1, 19-2 and Sonderforschungsbereich 555, part project B8). Most of the literature search has been performed with the ADS system.

Appendix A: The static solution without mixing

In order to discuss the possible existence of dust particles in a truly static atmosphere, we consider the dust moment and element consumption equations in the static stationary case (Eqs. (5) and (6)), i.e. without mixing. Concerning Eq. (6), both terms on the l.h.s. are negative in case of supersaturation and positive in case of undersaturation[14]. Since their sum is zero, each term must be zero, i.e.

$$J(V_\ell) = 0 \quad \text{and} \quad \Big\{ S = 1 \ \text{ or } \ L_2 = 0 \Big\}. \tag{A.1}$$

From the definition of the dust moments as integrals over a strictly positive size distribution function $f(V) \geq 0$, multiplied by some power of the positive volume $V^j \geq 0$, it is clear that $L_2 = 0$ implies $L_j = 0$ for all j. Furthermore, $S = 1$ implies that $\chi^{\rm net}_{\rm lKn} = 0$ according to Eq. (2). Consequently, Eq. (A.1) is equivalent to

$$J(V_\ell) = 0 \quad \text{and} \quad \Big\{ \chi^{\rm net}_{\rm lKn} = 0 \ \text{ or } \ L_j = 0 \Big\}. \tag{A.2}$$

Thus, the following conclusions can be drawn:

- $S < 1$: According to Eq. (2), undersaturation implies $\chi^{\rm net}_{\rm lKn} < 0$. We can hence conclude from Eq. (A.2) that the gas must be dust-free $L_j = 0$. This is the usual case of "normal" stellar atmospheres, where the gas is too hot for saturation and all dust particles have disappeared (if ever existed) due to evaporation.
- $S = 1$: Saturation implies $J(V_\ell) = 0$ and $\chi^{\rm net}_{\rm lKn} = 0$ according to Eq. (2). Inserting this result into the static dust moment equations (Eq. (5)), we can deduce that $\frac{\rm d}{{\rm d}z}({\rm d}L_j/c_{\rm T}) = 0$ for all j or
$$L_j = {\rm const}_j \cdot c_{\rm T} = {\rm const}_j \cdot \sqrt{2kT/\bar{\mu}}. \tag{A.3}$$
This solution describes the pure effect of drift on the dust moments, i.e. dust particles which drift through the atmosphere without changing their properties. However, at some depth in the atmosphere the gas must become undersaturated because of the inward increasing temperature. A continuous transition to the $S < 1$ case is hence only possible if ${\rm const}_j = 0$ for all j. Physically speaking, the dust particles cannot simply disappear at the borderline to $S < 1$, but have to evaporate there which would constantly enrich this layer with condensable elements – in contradiction to the assumption of a static atmosphere. We conclude that the gas must be dust-free also for $S = 1$.
- $S > 1$: This case contradicts the $J(V_\ell) = 0$ condition, because supersaturation always implies a possibly very small but in any case non-vanishing nucleation rate.

Consequently, the gas cannot be supersaturated ($S \leq 1$) and must be dust-free ($L_j = 0$) in a truly static atmosphere. This solution is designated as *trivial solution*.

[14] As argued in Paper II, $S_r = S^{(m_r)}$ is valid for simple types of growth reactions, where m_r denotes the number of monomers of the solid compound created by that reaction. Therefore, e.g. $S > 1$ is equivalent to $S_r > 1$ for all r.

Appendix B: TiO_2 mean extinction efficiencies

Scaled extinction efficiencies $Q'(\lambda) = Q_{\rm ext}(a,\lambda)/a$ for solid TiO_2 (rutile) have been calculated from the complex refractory index $\boldsymbol{m}_\lambda$ in the small particle limit via

$$Q'(\lambda) = \frac{8\pi}{\lambda} \, {\rm Im}\left\{ \frac{\boldsymbol{m}_\lambda^2 - 1}{\boldsymbol{m}_\lambda^2 + 2} \right\}, \tag{B.1}$$

based on the optical constants kindly provided by Th. Posch (1999, priv. comm.). Monochromatic values of $Q'(\lambda)$ used for the $\Delta\tau$-estimations in Table 2 at $\lambda = 1.25\,\mu$m, $2.2\,\mu$m and $13.3\,\mu$m are $5.5\,{\rm cm}^{-1}$, $5.7\,{\rm cm}^{-1}$ and $75000\,{\rm cm}^{-1}$, respectively.

From these data, we have calculated Planck and Rosseland means, $Q'_{\rm Pl}(T)$ and $Q'_{\rm Ross}(T)\,[{\rm cm}^{-1}]$. The results as function of temperature T [K] can be fitted by

$$x = \log T \tag{B.2}$$

$$\log Q'_{\rm Pl}(T) = \sum_{i=0}^{5} c_i x^i \tag{B.3}$$

$$\log Q'_{\rm Ross}(T) = \Big(1 - \Gamma(x)\Big) \sum_{i=0}^{3} a_i x^i \ + \ \Gamma(x) \sum_{i=0}^{3} b_i x^i \tag{B.4}$$

$$\Gamma(x) = 1 \Big/ \Big(\exp\Big[d_1 \cdot (x - d_0) \Big] + 1 \Big) \tag{B.5}$$

with the fit coefficients shown in Table B.1.

Table B.1. Fit coefficients for the TiO_2 mean dust opacities. The fits are valid between 50 K and 3000 K.

i	d_i	a_i	b_i	c_i
0	2.356980	35.090799	−2.647117	77.824722
1	12.297591	−30.181877	1.998290	−182.476022
2		8.856967	−0.104436	159.611494
3		−0.867332	0.052844	−64.837441
4				12.516761
5				−0.935180

References

Ackermann, S., & Marley, M. 2001, ApJ, 556, 872

Allard, F., Hauschildt, P., Alexander, D., Tamanai, A., & Schweitzer, A. 2001, ApJ, 556, 357

Burgasser, A., Marley, M., Ackerman, A., et al. 2002, ApJ, 571, L151

Burrows, A., & Sharp, C. M. 1999, ApJ, 512, 843

Burrows, A., Burgasser, A., Kirkpatrick, J., et al. 2002, ApJ, 573, 394

Chabrier, G., & Baraffe, I. 1997, A&A, 327, 1039

Chase Jr., M. W., Davies, C. A., Downey Jr., J. R., et al. 1985, JANAF Thermochemical Tables (National Bureau of Standards)

Cooper, C. S., Sudarsky, D., Milsom, J. A., Lunine, J. I., & Burrows, A. 2003, ApJ, 586, 1320

Deuflhard, P., & Wulkow, M. 1989, IMPACT Comp. Sci. Eng., 1, 269

Dominik, C., Sedlmayr, E., & Gail, H.-P. 1993, A&A, 277, 578

Feder, J., Russell, K. C., Lothe, J., & Pound, G. M. 1966, Adv. Phys., 15, 111

Freytag, B., Ludwig, H.-G., & Steffen, M. 1996, A&A, 313, 497

Gail, H.-P., & Sedlmayr, E. 1988, A&A, 206, 153

Gail, H.-P., Keller, R., & Sedlmayr, E. 1984, A&A, 133, 320

Gauger, A., Gail, H.-P., & Sedlmayr, E. 1990, A&A, 235, 345

Hairer, E., & Wanner, G. 1991, Solving Ordinary Differential Equations II (Berlin: Springer)

Helling, Ch., Winters, J. M., & Sedlmayr, E. 2000, A&A, 358, 651

Helling, Ch., Oevermann, M., Lüttke, M., Klein, R., & Sedlmayr, E. 2001a, A&A, 376, 194

Helling, Ch., Lüttke, M., Sedlmayr, E., & Klein, R. 2001b, in Freistühler W., Hyperbolic Problems: Theory – Numeric – Applications (Birkhäuser), 515

Jeong, K. S. 2000, Dust shells around oxygen–rich Miras and long–period variables, Ph.D. Thesis, Technische Universität, Berlin, Germany

Jeong, K. S., Chang, C., Sedlmayr, E., & Sülzle, D. 2000, J. Phys. B, 33, 3417

Kirkpatrick, J. D., Reid, I. N., Liebert, J., et al. 1999, ApJ, 519, 802

Kufuß, R. 1987, Ein Modell für zeitabhängige Konvektion in Sternen, Ph.D. Thesis, TU München

Leggett, S. K., Allard, F., Geballe, T. R., Hauschildt, P. H., & Schweitzer, A. 2001, ApJ, 548, 908

Ludwig, H.-G. 2003, in Modelling of Stellar Atmospheres, ed. N. E. Piskunov, W. W. Weiss, & D. F. Gray, IAU Symp., 210, in press

Ludwig, H.-G., Allard, F., & Hauschildt, P. H. 2002, A&A, 395, 99

Lunine, J. I., Hubbard, W. B., Burrows, A., Wang, Y.-P., & Garlow, K. 1989, ApJ, 338, 314

Marley, M., Seager, S., Saumon, D., et al. 2002, ApJ, 568(1), 335

Meneveau, C., & Katz, J. 2000, Annu. Rev. Fluid Mech., 32, 1

Patzer, A. B. C., Chang, C., Sedlmayr, E., & Sülzle, D. 1999, Eur. Phys. J. D, 6, 57

Pijpers, F. P., & Habing, H. J. 1989, A&A, 215, 334

Rossow, W. V. 1978, Icarus, 36, 1

Sengupta, S. 2003, ApJ, 585, L155

Sengupta, S., & Krishan, V. 2001, ApJ, 561, L123

Tsuji, T. 2002, ApJ, 575, 264

Woitke, P. 1999, in Astronomy with Radioactivities, 163–174, MPE Report 274, ed. R. Diehl, & D. Hartmann (Germany: Schloß Ringberg)

Woitke, P., & Helling, Ch. 2003, A&A, 399, 297 (Paper II)

Wuchterl, G., & Tscharnuter, W. M. 2003, A&A, 398, 1081

Wulkow, M. 1992, IMPACT Comp. Sci. Eng., 4, 153